

Quantification of N-acetylcysteine in drug formulations using inhibitory kinetic spectrophotometric method

Basant LAL^{1*}, Abhas ASTHANA², Vinay Kumar SINGH³, Krishna SRIVASTAVA⁴

¹ Department of Chemistry, GLA University, Mathura- 281406, U.P., India

² Department of Chemistry, M.J.S. Government P.G. College, Bhind, M.P., India

³ Department of Chemistry, Dr. Shakuntala Misra National Rehabilitation University, Lucknow, U.P., India

⁴ Department of Chemistry, Shri Ramswaroop Memorial University, Barabanki, 222502, U.P., India.

* Corresponding Author. E-mail: basant.lal@gla.ac.in (B.L.); Tel. +91- 9690512647

Received: 18 May 2022 / Revised: 16 July 2022 / Accepted: 17 July 2022

ABSTRACT: A simple, reproducible, and rapid kinetic method for the N-acetylcysteine (NAC) determination has been proposed and linked to NAC quantification in pharmaceutical preparations. The method is based on the inhibitory feature of N-acetylcysteine. NAC forms a stable complex with Hg^{2+} and reduces the actual Hg^{2+} concentration and ultimately the rate of reaction between pyrazine (Pz) and $[Ru(CN)_6]^{4-}$ catalyzed by Hg^{2+} . Under the optimized reaction conditions with $[Ru(CN)_6]^{4-} = 7.25 \times 10^{-5}$ mole dm^{-3} , $I = 0.1$ mole dm^{-3} (KCl), Temp = 45.0 ± 0.1 °C, $[Hg^{2+}] = 1.5 \times 10^{-4}$ mole dm^{-3} , $[Pyrazine] = 8.5 \times 10^{-4}$ mole dm^{-3} , and pH = 4.0 ± 0.02 , fixed time of 12 and 17 min was selected to compute the absorbance at 370 nm corresponding to the ultimate reaction product $[Ru(CN)_5 Pz]^{3-}$. The inhibitory action of NAC towards cyanide imitation by pyrazine from $[Ru(CN)_6]^{4-}$, catalyzed by Hg^{2+} has been demonstrated by a redesigned mechanistic scheme. With the proposed kinetic spectrophotometric method, the micro level quantification of NAC in distinct water samples can be done down to 1.5×10^{-6} mole dm^{-3} . The developed procedure is highly reproducible and can be efficiently used to quantitatively estimate the NAC in the drug samples with high accuracy. The general additives present in drugs do not substantially interfere in the determination of NAC even up to 1000 times with [NAC].

KEYWORDS: Hexacyanoruthenate(II); pharmaceutical preparations; excipients; catalyst inhibitor complex; N-acetylcysteine; ligand substitution reaction; inhibitory effect.

1. INTRODUCTION

N-acetylcysteine (NAC), a precursor of glutathione is a natural antioxidant found in onion. It is listed as an essential medicine in the World Health Organization (WHO) model list since 1960. N-acetylcysteine is used for the treatment of the overdose of paracetamol and to loosen the thicker mucus in individuals and with chronic bronchopulmonary disorders such as bronchitis and many more like pneumonia [1-4]. N-acetylcysteine itself or in conjugation with other supplements used as a dietary product in various psychiatric conditions [5]. As NAC slow down the blood-clotting, person having bleeding disorder or who takes blood-thinning medicines should not take it [6]. NAC is potentially effective in degenerative processes caused by aging [7].

For centuries, sulfur continues to be the dominating heteroatom in the wide varieties of FDA approved drugs and bioactive molecules. Organosulfur compounds play specific role in distinct metabolic process as enzyme and structural proteins [8-11]. Pharmaceutical industry is always looking towards the analytical chemists for the efficient methodology for the detection and quantification of sulfur bearing bioactive molecules and drugs in distinct samples. The fundamental importance and immediate applications of redox/ligand exchange reactions of transition metal complexes in synthetic, analytical, and organometallic chemistry attracted many chemists for their kinetic study [12-16]. Numerous kinetic reports on oxidation of Fe(II) / Co(II) complexes and cyanide substitution from cyano complexes of Fe(II) / Ru(II) are available in literature [17-19].

Different approaches for the quantification of thio compounds in biological, analytical and drug samples are often used [20-23]. The quantification methodology includes voltammetry [24], flow injection

How to cite this article: Lal B, Asthana A, Singh VK, Srivastava K. Quantification of N-acetylcysteine in drug formulations using inhibitory kinetic spectrophotometric method. J Res Pharm. 2022; 26(6): 1713-1722.

analysis [25], NMR-spectrometry [26], fluorimetry [27], colorimetry [20], chromatography [28-30], spectrophotometry [31, 32], and potentiometry [33]. The main drawbacks of above-mentioned methods may include high initial investment, time-consuming process, heavy instrumentation, and high cost for sample analysis. Very few reports are available on kinetic spectrophotometric method, which require only UV-Visible spectrophotometer for drug quantification [34-36].

Bioactive ruthenium complexes exhibit wide range applications as antiamebic [37], immunosuppressant [38], DNA binder [39], antifungal [40], antileukemic [41], antimetastatic [42], antitumor [43] and anticancer [44]. The metal catalyzed Hg(II) / Ag(I), cyanide substitution from cyano complexes of Fe(II) / Ru(II) by heterocyclic ligand containing nitrogen have been reported by several authors [19, 45]. These reactions have also been successfully used for the micro level determination of employed catalyst and drugs / compounds that can bind strongly with catalyst. Organosulfur compounds form a stable complex with Hg(II), thereby decreasing the cyanide substitution to a considerable extent as the organosulfur compounds substantially inhibit the catalytic efficacy of Hg(II). This inhibitory feature of thio compounds (with sulfur as -S-, -SH and S-) can be used for its trace level quantification using kinetic spectrophotometric method. NAC also reduces the catalytic efficacy of Hg(II), thereby decreasing the Hg(II) catalyzed rate of cyanide substitution with pyrazine from $[\text{Ru}(\text{CN})_6]^{4-}$.

More authentic result will be observed with the reaction in hand as the uncatalyzed reaction between pyrazine and $[\text{Ru}(\text{CN})_6]^{4-}$ was not noticed under the studied reaction condition. Because of the strong inhibitory action of NAC towards the catalytic efficacy of Hg(II), we conceived a simple, reproducible, and rapid kinetic spectrophotometric approach for the micro level quantification of NAC in distinct water samples down to 1.5×10^{-6} mole dm^{-3} . The current system is also employed for the quick quantification of NAC in drug samples with high reproducibility and good accuracy.

In this section, the authors should state the objectives of the work, define the scope of your paper, summarize relevant work to the study being reported and provide an adequate background. A detailed literature survey or a summary of the results should be avoided. It should not be a review of the subject area, but should finish with a clear statement of the question being addressed. The introduction must be designed to inform the reader of the rationale and significance of the study. Do not leave blank lines or paragraph spacing between the adjacent paragraphs.

2. RESULTS AND DISCUSSION

The final reaction product $[\text{Ru}(\text{CN})_5 \text{Pz}]^{3-}$ is formed by the Hg(II) catalyzed reaction between pyrazine and $[\text{Ru}(\text{CN})_6]^{4-}$. During the reaction $[\text{Ru}(\text{CN})_6]^{4-}$ and pyrazine reacts in 1:1 mole ratio that was confirmed by mole ratio and slope ratio examination of final reaction product. Since the all reacting solutions except the final reaction product exhibit no appreciable absorption at the studied wave length, no correction in the absorption values were applied [45]. The strong absorption band at 370 nm (spectra not represented) belongs to the final product $[\text{Ru}(\text{CN})_5 \text{Pz}]^{3-}$ and is due to the metal to ligand charge transfer (MLCT) complex.

The preceding literature on D- penicillamine, thioglycolic acid, sodium thiosulphate, methionine, and carbocysteine admit that the sulfur compounds reduces the rate of Hg(II) catalyzed reaction between nitrogen donor ligand and $[\text{Ru}(\text{CN})_6]^{4-}$ [34-36, 46-49]. The observed reduced rate is due to the formation of stable complex by added sulfur compounds with Hg(II), which eventually reduces the active concentration of Hg(II). NAC forms a stable complex with Hg^{2+} and reduces the actual Hg^{2+} concentration and ultimately the rate of reaction between pyrazine and $[\text{Ru}(\text{CN})_6]^{4-}$ catalyzed by Hg^{2+} . Figure 1 exhibits the structure of N-acetylcysteine.

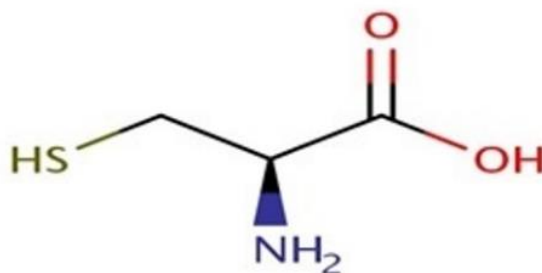


Figure 1. Structure of N-acetylcysteine [NAC]

The absorbance (A_t), corresponding to the ultimate reaction product $[\text{Ru}(\text{CN})_5 \text{Pz}]^{3-}$, with varying $[\text{NAC}]$ was computed at fixed time (12 and 17 min after mixing of reactants). A plot (calibration curve) of absorbance versus $[\text{NAC}]$, found to be linear in 1.5×10^{-6} - 5.35×10^{-5} mole dm^{-3} concentration range of NAC, did the quantification of NAC (Figure 2). The regression line relating A_t and $[\text{NAC}]$ can be expressed as Eq.1 and 2.

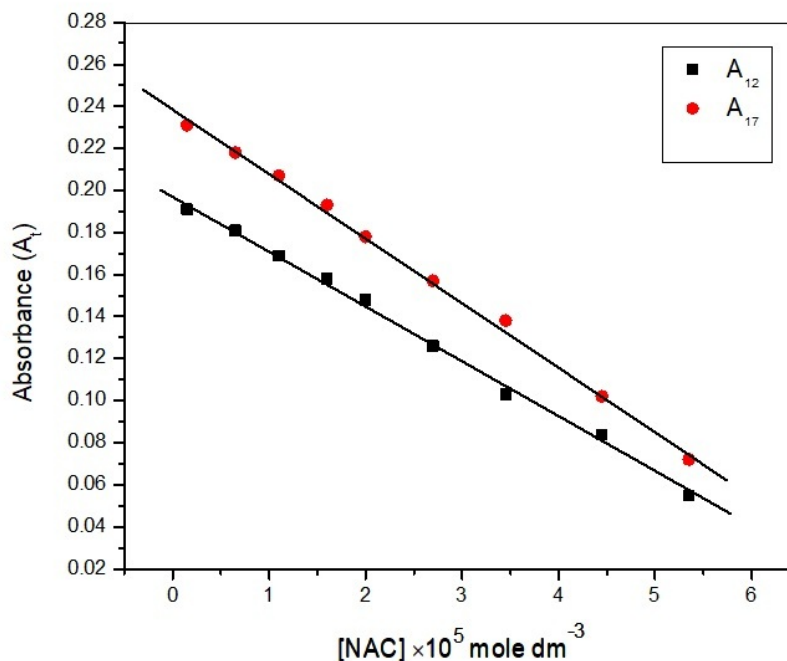


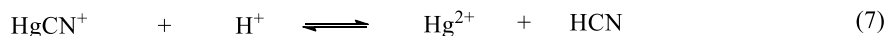
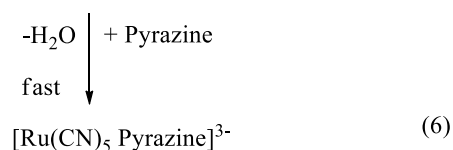
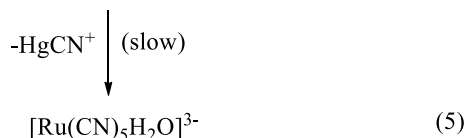
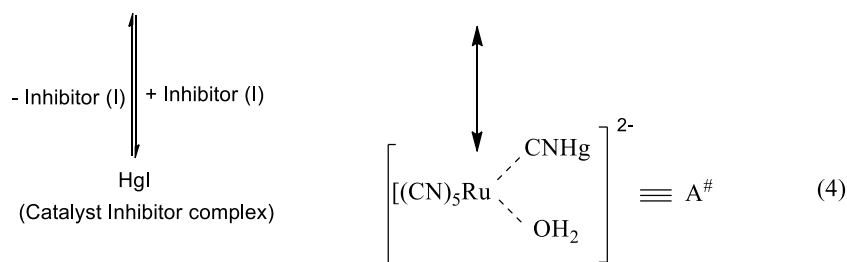
Figure 2. Calibration curve for quantification of N-acetylcysteine at $[\text{Ru}(\text{CN})_6^{4-}] = 7.25 \times 10^{-5}$ mole dm^{-3} , $I = 0.1$ mole dm^{-3} (KCl), Temp = 45.0 ± 0.1 °C, $[\text{Hg}^{+2}] = 1.5 \times 10^{-4}$ mole dm^{-3} , $[\text{Pyrazine}] = 8.5 \times 10^{-4}$ mole dm^{-3} , and pH = 4.0 ± 0.02

$$A_{12} = 0.198 - 2.64 \times 10^3 [\text{NAC}] \quad (1)$$

$$A_{17} = 0.239 - 3.06 \times 10^3 [\text{NAC}] \quad (2)$$

The calculated value of linear regression coefficient and standard deviation for A_{12} and A_{17} plot (A_t versus $[\text{NAC}]$) was 0.9953, 0.9976 and 0.0026, 0.0028 respectively. The absorbance (after 12 min.) was noted down after adding calculated amount of NAC to the reaction system. By calibration curve (Figure 2) the value of recovered NAC was calculated (Table 1). Recovered NAC confirmed the reproducibility and accuracy of the reported method.

The inhibitory action of NAC towards cyanide imitation from $[\text{Ru}(\text{CN})_6]^{4-}$ by pyrazine, catalyzed by Hg^{2+} has been demonstrated by a redesigned mechanistic scheme (equations 3 - 7). More authentic result will be observed with the reaction in hand as the uncatalyzed reaction between pyrazine and $[\text{Ru}(\text{CN})_6]^{4-}$ was not noticed under the studied reaction condition [45].



Considering hexacyanoruthenate(II) as a single substrate with initial concentration S_0 . In the presence of inhibitor (NAC), the catalyzed reaction rate can be deduced parallel to the enzyme-catalyzed reaction. Equation 8 represents the rate of catalyzed reaction (V_o) in the deflection of NAC.

$$V_o = \frac{V_{\max}}{1 + \frac{K_m}{[S_0]}} \quad (8)$$

Here K_m and V_{\max} give maximum rate at larger reactant concentration and Michaelis-Menten constant respectively. The straight-line form ($1/V_o$ versus $1/[S_0]$) of the above equation having intercept and slope $1/V_{\max}$ and K_m/V_{\max} respectively, represented by Eq. 9, is in accordance with Lineweaver-Burk expression [50].

Table 1: Recovery results for NAC quantification

[NAC]×10 ⁵ mole dm ⁻³ (Taken)	A ₁₂		A ₁₇	
	[NAC]×10 ⁵ mole dm ⁻³ (Found)	Error	[NAC]×10 ⁵ mole dm ⁻³ (Found)	Error
0.45	0.46 ± 0.029	+ 0.022	0.47 ± 0.046	+ 0.044
0.65	0.65 ± 0.03	0.000	0.64 ± 0.05	- 0.015
1.40	1.41 ± 0.038	+ 0.007	1.40 ± 0.00	0.000
1.80	1.78 ± 0.06	- 0.011	1.75 ± 0.042	- 0.028
2.30	2.30 ± 0.00	0.000	2.28 ± 0.06	- 0.009
3.05	3.08 ± 0.040	+ 0.01	3.09 ± 0.03	+ 0.013
3.80	3.76 ± 0.073	- 0.011	3.81 ± 0.068	+ 0.003
4.55	4.59 ± 0.057	+ 0.009	4.51 ± 0.042	- 0.009

Reaction Condition: $[\text{Ru}(\text{CN})_6^{4-}] = 7.25 \times 10^{-5}$ mole dm⁻³, $I = 0.1$ mole dm⁻³ (KCl), Temp = 45.0 ± 0.1 °C, $[\text{Hg}^{2+}] = 1.5 \times 10^{-4}$ mole dm⁻³, $[\text{Pyrazine}] = 8.5 \times 10^{-4}$ mole dm⁻³, and pH = 4.0 ± 0.02

$$\frac{1}{V_o} = \frac{1}{V_{\max}} + \frac{K_m}{V_{\max}} \frac{1}{[S_0]} \quad (9)$$

The K_m value calculated using slope and intercept of Figure 3 was 0.4967 ± 0.0272 mM.

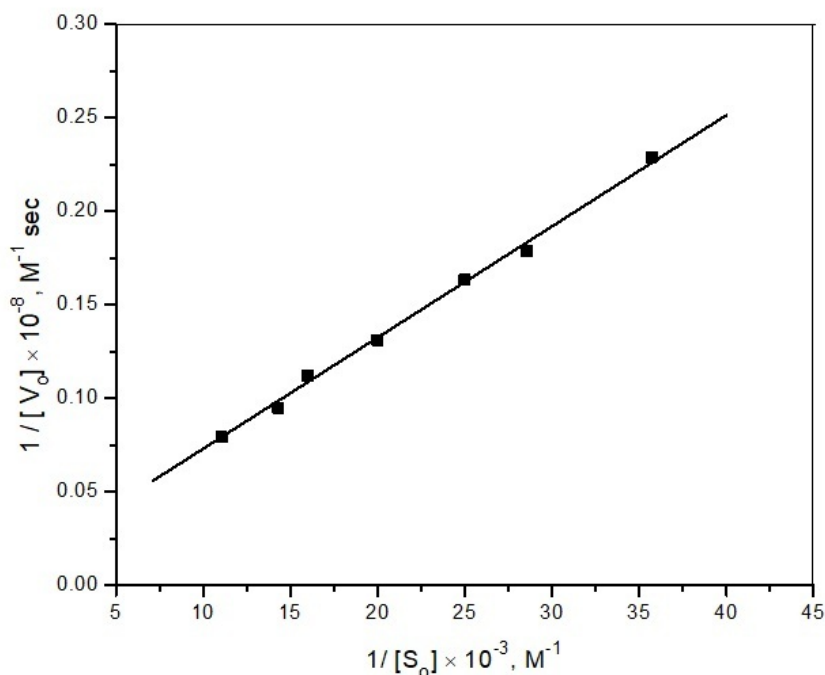


Figure 3. The Lineweaver-Burk plot at constant $[Hg^{2+}]$ in the absence of NAC at $I = 0.1$ mole dm^{-3} (KCl), $Temp = 45.0 \pm 0.1$ °C, $[Hg^{2+}] = 1.5 \times 10^{-4}$ mole dm^{-3} , $[Pyrazine] = 8.5 \times 10^{-4}$ mole dm^{-3} , and $pH = 4.0 \pm 0.02$

The apparent M-M constant " K'_m ", in the inhibitor's presence, at constant catalyst concentration can be represented as:

$$K'_m = K_m \left(1 + \frac{[I_0]}{K'_{CI}} \right)$$

Where K'_{CI} corresponds to the catalyst-inhibitor complex's (C-I) dissociation constant while initial [NAC] is represented by I_0 . The initial rate (V_i) in the inhibitor's presence, at constant catalyst concentration can be represented by Eq. 10 [51].

$$V_i = \frac{V_{max}}{1 + \frac{K'_m}{[S_0]}} \quad (10)$$

$$V_i = \frac{V_{max}}{1 + \frac{K_m}{[S_0]} \left(1 + \frac{[I_0]}{K'_{CI}} \right)} \quad (11)$$

The straight-line form of Eq. 11 in accordance to Lineweaver-Burk equation can be given as Eq. 12.

$$\frac{1}{V_i} - \frac{1}{V_{max}} = \frac{K_m}{[S_0]V_{max}} + \frac{K_m}{[S_0]V_{max}} \frac{[I_0]}{K'_{CI}} \quad (12)$$

The intercept and slope of the linear plot between $\left(\frac{1}{V_i} - \frac{1}{V_{max}}\right)$ and initial [NAC] was used to determine the K'_{CI} and K_m (in the presence of NAC) value and were found to be $4.21 \times 10^{-5} \pm 0.18$ and 0.4943 ± 0.0208 mM respectively (Figure 4). The calculated K_m value in the presence and absence of NAC is almost same. The lower dissociation constant value ($4.21 \times 10^{-5} \pm 0.18$) suggests the highly stable nature of catalyst inhibitor complex.

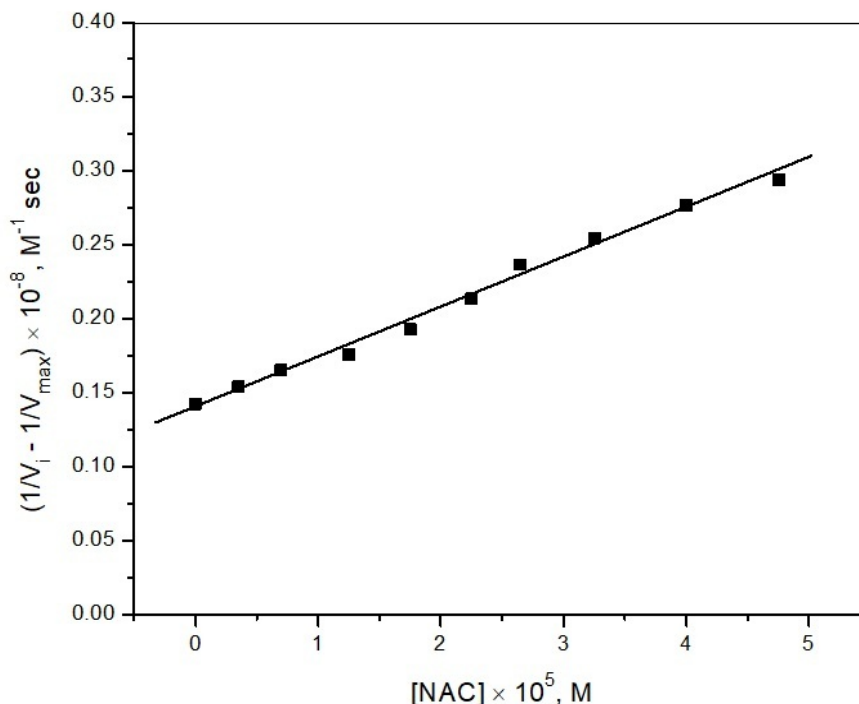


Figure 4. The plot of $(1/V_i - 1/V_{max})$ versus initial $[NAC]$ at $[Ru(CN)_6^{4-}] = 7.25 \times 10^{-5}$ mole dm^{-3} , $I = 0.1$ mole dm^{-3} (KCl), $Temp = 45.0 \pm 0.1$ °C, $[Hg^{2+}] = 1.5 \times 10^{-4}$ mole dm^{-3} , $[Pyrazine] = 8.5 \times 10^{-4}$ mole dm^{-3} , and $pH = 4.0 \pm 0.02$

3.1 Interference of co-existing components

Excipients, other than the active pharmaceutical ingredient are the inert compounds that are used as the vehicle, preservatives, coloring agents and fillers in pharmaceutical preparations. Optimized reaction conditions using the A_{12} calibration curve, containing $4.0 \mu gml^{-1}$ NAC and large number of distinct excipients was utilized to check the influence of excipients by performing recovery experiments. The recovery results show that the general additives present in drugs do not substantially interfere in the determination of NAC even up to 1000 times with $[NAC]$ (Table 2).

Table 2: NAC Recovery results in the presence of excipients

Additives	[Additives]/ [NAC]	Recovery ± SD (%)
Maltitol	1000	100.3 ± 0.4
Sorbitol	500	99.7 ± 0.6
Citrate	500	100.4 ± 0.2
Sucrose	1000	99.2 ± 0.8
Magnesium stearate	500	100.2 ± 0.3
Lactose	1000	100.8 ± 0.6
Sodium Lauril sulphate	1000	99.6 ± 0.5
Gelatin	500	99.3 ± 0.7

Reaction Conditions: $[Ru(CN)_6^{4-}] = 7.25 \times 10^{-5}$ mole dm^{-3} , $I = 0.1$ mole dm^{-3} (KCl) $Temp = 45.0 \pm 0.1$ °C, $[Hg^{2+}] = 1.5 \times 10^{-4}$ mole dm^{-3} , $[Pyrazine] = 8.5 \times 10^{-4}$ mole dm^{-3} , and $pH = 4.0 \pm 0.02$

3.2 Application in pharmaceutical preparations

The quantitative determination of NAC in various drug samples was done by the suggested kinetic spectrophotometric method, for that the ground content of 10 tablet/capsule was dissolved in double distilled water (100 ml). The solution thus obtained was sonicated for 20 min, after filtration via Whatman filter paper the dilution of solution was done to bring drug concentration within the A_{12} calibration range.

Five different drugs containing only NAC and excipients, obtained from local drug dealer were applied to the suggested kinetic method for the quantification of NAC. The obtained result is compared with the official method (Table 3) [52]. The statistical comparison and mean recovery (99-101) results demonstrate the replicability and accuracy of the proposed method for the NAC quantification in water samples and drug formulations.

Table 3: NAC quantification in drug samples and comparison with the official method

Pharmaceutical Samples	Proposed Method Recovery \pm SD (%)	Official Method Recovery \pm SD (%)
Munex 600 Mg Tablet (Reckitt Benckiser India Limited, New Delhi)	99.69 \pm 0.68	99.62 \pm 0.75
Cysklis 600 Mg Tablet (APA Pharmaceuticals, Chandigarh)	101.08 \pm 0.59	100.71 \pm 0.49
Mucomix 600 Mg Capsule (Samarth Life Sciences Pvt Ltd, Mumbai)	99.94 \pm 0.73	98.94 \pm 0.38
Mucobet 300 Mg Tablet (Edolf Healthcare Private Limited)	100.76 \pm 0.72	101.54 \pm 0.51
Acetynet 600 Mg Tablet (Care Formulation Labs Pvt Ltd, New Delhi)	99.46 \pm 0.52	100.52 \pm 0.68

Reaction Conditions: $[\text{Ru}(\text{CN})_6^{4-}] = 7.25 \times 10^{-5} \text{ mole dm}^{-3}$, $I = 0.1 \text{ mole dm}^{-3}$ (KCl) Temp = $45.0 \pm 0.1 \text{ }^\circ\text{C}$, $[\text{Hg}^{2+}] = 1.5 \times 10^{-4} \text{ mole dm}^{-3}$, $[\text{Pyrazine}] = 8.5 \times 10^{-4} \text{ mole dm}^{-3}$, and pH = 4.0 ± 0.02

*Data represented is the average of three kinetic run

3. CONCLUSION

A new rapid, simple and highly reproducible kinetic method, based on the inhibitory property of sulfur bearing compound NAC towards Hg(II) have been proposed for the quantitative estimation of NAC. Since under the studied conditions, pyrazine and hexacyanoruthenate(II) do not undergo any chemical reaction in the absence of Hg(II), the reaction system under investigation produces more accurate results for NAC determination. The general additives present in drugs do not substantially interfere in the determination of NAC even up to 1000 times with [NAC]. With the proposed kinetic spectrophotometric method, the micro level quantification of NAC in distinct water samples can be done down to $1.5 \times 10^{-6} \text{ mole dm}^{-3}$. The current system was also employed for the quick quantification of NAC in drug samples. The statistical comparison and mean recovery (99-101) results demonstrate the replicability and accuracy of the proposed method for the quantification of NAC in water samples and drug formulations. The methodology can be effectively used for the trace level determination of various drugs and biological molecules that can significantly inhibit the catalytic efficacy of Hg(II).

4. MATERIALS AND METHODS

4.1 Chemicals Used

Analytical grade reagents and double deionized water was utilized through the whole kinetic study. To prevent the possible photo-degradation of pyrazine (Merck) and $\text{K}_4[\text{Ru}(\text{CN})_6] \cdot 3\text{H}_2\text{O}$ (Sigma-Aldrich), their stock solution were kept in amber colored bottles. N-acetylcysteine was purchased from Sigma-Aldrich and was used as supplied. HgCl_2 (Merck) solution was prepared daily as it may be adsorbed on glass surface. Potassium hydrogen phthalate (Himedia) and HCl / NaOH (CDH Fine Chemicals) was applied to control the pH of the reaction medium while to regulate ionic strength of the reaction mixture KCl (Merck) was used.

4.2 Instrumentation and Kinetic Procedure

The pH of the reacting solutions was checked by Oakton digital benchtop pH meter model WW-35419-10, calibrated with predefined buffer solution. To record the absorbance at 370 nm corresponding to the ultimate reaction product $[\text{Ru}(\text{CN})_5 \text{Pz}]^{3-}$, A51119500C Multiskan Sky High Microplate Spectrophotometer (ThermoFisher Scientific) was used. Since the all reacting solutions except the final reaction product do not exhibit appreciable absorption at the studied wave length, no correction in the absorption values were

applied. From the detailed, kinetic study of the reaction, an ideal reaction condition was judiciously selected that exhibit significant absorption change at 370 nm [45]. After thermal equilibration (for 30 min at 45 °C) of all the reacting solution viz., $[\text{Ru}(\text{CN})_6^{4-}] = 7.25 \times 10^{-5} \text{ mole dm}^{-3}$, $\text{KCl} = 0.1 \text{ mole dm}^{-3}$, $[\text{Hg}^{2+}] = 1.5 \times 10^{-4} \text{ mole dm}^{-3}$, $[\text{Pyrazine}] = 8.5 \times 10^{-4} \text{ mole dm}^{-3}$, buffer of $\text{pH} = 4.0 \pm 0.02$, and NAC they are mixed promptly in the order: Pyrazine, HgCl_2 , buffer solution, KCl, NAC, and $[\text{Ru}(\text{CN})_6^{4-}]$. After brisk shaking, the reacting solution was promptly transported to the temperature controlled spectrophotometric cell. The temperature of the cell compartment was managed by self-designed circulating water arrangement system. The surge in absorbance corresponding to the ultimate product was recorded at fixed time. A plot (calibration curve) of absorbance versus varying $[\text{NAC}]$ did the quantification of NAC.

Author contributions: Concept - B.L., V.K.; Design - B.L., A.A., V.K.; K.S.; Supervision - B.L.; Resources - B.L., A.A.; Materials - V.K.; K.S.; Data Collection and/or Processing - B.L., A.A.; Analysis and/or Interpretation - B.L., A.A., V.K., K.S.; Literature Search - B.L., A.A., V.K.; K.S.; Writing - B.L.; V.K.; Critical Reviews - B.L., A.A., V.K., K.S.

Conflict of interest statement: None of the authors has any potential or actual conflict of interest to disclose in relation to the published article.

REFERENCES

- [1] Waring WS. Novel acetylcysteine regimens for treatment of paracetamol overdose. *Ther Adv Drug Saf.* 2012; 3(6): 305-315.
- [2] Hoffman RS. Acetylcysteine for paracetamol: Will one size ever fit all? *EClinicalMedicine.* 2020; 20: 100314. [\[CrossRef\]](#)
- [3] Bateman DN, Dear JW. Acetylcysteine in paracetamol poisoning: a perspective of 45 years of use. *Toxicol Res.* 2019; 8(4): 489-498. [\[CrossRef\]](#)
- [4] Sadowska AM, Verbraecken J, Darquennes K, De Backer WA. Role of N-acetylcysteine in the management of COPD. *Int J Chron Obstruct Pulmon Dis.* 2006; 1(4): 425-434. [\[CrossRef\]](#)
- [5] Šalamon S, Kramar B, Marolt TP, Poljšak B, Milisav I. Medical and Dietary Uses of N-Acetylcysteine. *Antioxidants (Basel).* 2019; 8(5): 111. [\[CrossRef\]](#)
- [6] Tardiolo G, Bramanti P, Mazzon E. Overview on the Effects of N-Acetylcysteine in Neurodegenerative Diseases. *Molecules.* 2018; 23: 3305. [\[CrossRef\]](#)
- [7] Craver BM, Ramanathan G, Hoang S, Chang X, Laura F, Luque M, Brooks S, Yeng Lai HY, Fleischman AG. N-acetylcysteine inhibits thrombosis in a murine model of myeloproliferative neoplasm. *Blood Adv.* 2020; 4(2): 312-321. [\[CrossRef\]](#)
- [8] Tang K. Chemical diversity and biochemical transformation of biogenic organic sulfur in the ocean. *Front Mar Sci.* 2020; 7: 68. [\[CrossRef\]](#)
- [9] Abadie C, Tcherkez G. Plant sulphur metabolism is stimulated by photorespiration. *Commun Biol.* 2019; 2: 379. [\[CrossRef\]](#)
- [10] Kolluru GK, Shen X, Kevil CG. Reactive sulfur species: a new redox player in cardiovascular pathophysiology. *Arterioscler Thromb Vasc Biol.* 2020; 40: 874-884. [\[CrossRef\]](#)
- [11] Fukuto JM, Ignarro LJ, Nagy P, Wink DA, Kevil CG, Feelisch M, Cortese-Krott MM, Bianco CL, Kumagai Y, Hobbs AJ. Biological hydropersulfides and related polysulfides-a new concept and perspective in redox biology. *FEBS Lett.* 2018; 592: 2140-2152. [\[CrossRef\]](#)
- [12] Omondi RO, Stephen O, Ojwach SO, Jaganyi D. Review of comparative studies of cytotoxic activities of Pt(II), Pd(II), Ru(II)/(III) and Au(III) complexes, their kinetics of ligand substitution reactions and DNA/BSA interactions. *Inorg Chim Acta.* 2020; 512: 119883. [\[CrossRef\]](#)
- [13] Naik RM, Srivastava A, Asthana A. The kinetics and mechanism of oxidation of hexacyanoferrate(II) by periodate ion in highly alkaline aqueous medium. *J Iran Chem Soc.* 2008; 5: 29-36. [\[CrossRef\]](#)
- [14] Iioka T, Takahashi S, Yoshida Y, Matsumura Y, Hiraoka S, Sato H. A kinetics study of ligand substitution reaction on dinuclear platinum complexes: Stochastic versus deterministic approach. *J Comput Chem.* 2019; 40: 279-285. [\[CrossRef\]](#)
- [15] Naik RM, Srivastava A, Verma AK, Yadav SBS, Singh R, Prasad S. The kinetics and mechanism of oxidation of triethylenetetraaminehexaacetate. *Bioinorg Reac Mech.* 2007; 6: 185-192. [\[CrossRef\]](#)
- [16] Srivastava A, Sharma V, Prajapati A, Srivastava N, Naik RM. Spectrophotometric determination of ruthenium utilizing its catalytic activity on oxidation of hexacyano ferrate(II) by periodate ion in water samples. *Chem Chem Technol.* 2019; 13(3): 275-279. [\[CrossRef\]](#)
- [17] Naik RM, Srivastava A, Verma AK. The kinetics and mechanism of ruthenium(iii)-catalyzed oxidation of tris(2-amino ethyl)amine by hexacyanoferrate(iii) in aqueous alkaline medium. *Turk J Chem.* 2008; 32(4): 495-503.
- [18] Rastogi R, Srivastava A, Naik RM. Kinetic and mechanistic analysis of ligand substitution of aquapentacyanoruthenate(II) in micelle medium by nitrogen donor heterocyclic ligand. *J Disp Sc Tech.* 2020; 41(7): 1045-1050. [\[CrossRef\]](#)

- [19] Srivastava A, Naik RM, Rastogi R. Spectrophotometric kinetic study of mercury(II) catalyzed formation of [4-CN-PyRu(CN)₅]³⁻ via ligand exchange reaction of hexacyanoruthenate(II) with 4-cyanopyridine - a mechanistic approach. *J Iran Chem Soc.* 2020; 17(9): 2327-2333. [CrossRef]
- [20] Tanwar J, Datta A, Chauhan K, Kumaran SS, Tiwari AK, Kadiyala KG, Pal S, Thirumal M, Mishra AK. Design and synthesis of calcium responsive magnetic resonance imaging agent: Its relaxation and luminescence studies. *Eur J Med Chem.* 2014; 82: 225-232. [CrossRef]
- [21] Saini N, Varshney R, Tiwari AK, Kaul A, Allard M, Ishar MP, Mishra AK. Synthesis, conjugation and relaxation studies of gadolinium(III)-4-benzothiazol-2-yl-phenylamine as a potential brain specific MR contrast agent. *Dalton Trans.* 2013; 42(14): 4994-5003. [CrossRef]
- [22] Kostara A, Tsogas GZ, Vlessidis AG, Giokas DL. Generic assay of sulfur-containing compounds based on kinetics inhibition of gold nanoparticle photochemical growth. *ACS Omega.* 2018; 3(12): 16831-16838. [CrossRef]
- [23] Raab A, Feldmann J. Biological sulphur-containing compounds - Analytical challenges. *Anal Chim Acta.* 2019; 1079: 20-29. [CrossRef]
- [24] Shoba S, Bankole OM, Ogunlaja AS. Electrochemical determination of trace sulfur containing compounds in model fuel based on a silver/polyaniline-modified electrode. *Anal Methods.* 2020; 12: 1094-1106. [CrossRef]
- [25] Perez-Ruiz T, Martinez-Lozano C, Tomas V, Sidrach-de-cardona C. Flow-injection fluorimetric determination of penicillamine and tiopronin in pharmaceutical preparations. *J Pharm Biomed Anal.* 1996; 15: 33-38. [CrossRef]
- [26] Nelson J. Nuclear magnetic resonance spectroscopic method for determination of penicillamine in capsules. *J Assoc Off Anal Chem.* 1981; 64: 1174-1178. [CrossRef]
- [27] Nugrahani I, Abotbina IM, Apsari CN, Kartavinata TG, Sukranso Oktaviary R. Spectrofluorometric determination of L-tryptophan in canary (*Canarium indicum* L.) seed protein hydrolysate. *Biointerface Res Appl Chem.* 2019; 10(1): 4780-4785. [CrossRef]
- [28] Feng G, Sun S, Wang M, Zhao Q, Liu L, Hashi Y, Jia R. Determination of four volatile organic sulfur compounds by automated headspace technique coupled with gas chromatography-mass spectrometry. *J Water Supply Res T.* 2018; 67(5): 498-505. [CrossRef]
- [29] Dzieko U, Kubczak N, Przybylska KP, Patalski P, Balcerek M. Development of the method for determination of volatile sulfur compounds (vscs) in fruit brandy with the use of HS-SPME/GC-MS. *Molecules.* 2020; 25: 1232. [CrossRef]
- [30] Cao L, Wei T, Shi Y, Tan X, Meng J. Determination of D-penicillamine and tiopronin in human urine and serum by HPLC-FLD and CE-LIF with 1,3,5,7-tetramethyl-8-bromomethyl-difluoroboradiaza-s-indacene. *J Liq Chrom Relat Tech.* 2018; 41(2): 58-65. [CrossRef]
- [31] Pooja, Singh D, Aggarwal S, Singh VK, Pratap R, Mishra AK, Tiwari AK. Lanthanide (Ln³⁺) complexes of bifunctional chelate: Synthesis, physicochemical study and interaction with human serum albumin (HSA). *Spectrochim Acta A Mol Biomol Spectrosc.* 2021; 244: 118808. [CrossRef]
- [32] Ni L, Geng X, Li S, Ning H, Guan Y. A flame photometric detector with a silicon photodiode assembly for sulfur detection. *Talanta.* 2020; 207: 120283. [CrossRef]
- [33] Chao Q, Sheng H, Cheng X, Ren T. Determination of sulfur compounds in hydrotreated transformer base oil by potentiometric titration. *Ana Sci.* 2005; 21: 721-724. [CrossRef]
- [34] Srivastava A. Micro-level estimation of Mercaptoacetic acid using its inhibitory effect to mercury catalyzed ligand exchange reaction of hexacyanoruthenate(II). *Biointerface Res Appl Chem.* 2020; 10(6): 7152-7161. [CrossRef]
- [35] Agarwal A, Prasad S, Naik RM. Inhibitory kinetic spectrophotometric method for the quantitative estimation of D-penicillamine at micro levels. *Microchem J.* 2016; 128: 181-186. [CrossRef]
- [36] Srivastava A. Micro-level Estimation of Methionine Using Inhibitory Kinetic Spectrophotometric Method. *Biointerface Res Appl Chem.* 2021; 11(3): 10654-10663. [CrossRef]
- [37] Athar F, Husain K, Abid M, Azam A. Synthesis and anti-amoebic activity of gold(I), ruthenium(II), and copper(II) complexes of metronidazole. *Chem Biodiversity.* 2005; 2: 1320-1330. [CrossRef]
- [38] Bastos CM, Gordon KA, Ocain TD. Synthesis and immunosuppressive activity of ruthenium complexes. *Bioorg Med Chem Lett.* 1998; 8: 147-150. [CrossRef]
- [39] Yu B, Rees TW, Liang J, Jin C, Chen Y, Ji L, Chao H. DNA interaction of ruthenium(II) complexes with imidazo [4,5-f] [1,10] phenanthroline derivatives. *Dalton Trans.* 2019; 48: 3914-21. [CrossRef]
- [40] Gomes-Junior FA, Silva RS, Lima RG, Vannier-Santos MA. Antifungal mechanism of [RuIII(NH₃)₄catechol]⁺ complex on fluconazole-resistant *Candida tropicalis*. *FEMS Microbio Lett.* 2017; 364(9). [CrossRef]
- [41] Kenny RG, Marmion CJ. Toward multi-targeted platinum and ruthenium drugs - A new paradigm in cancer drug treatment regimens? *Chem Rev.* 2019; 119: 1058-1137. [CrossRef]
- [42] Gua L, Lia X, Ran Q, Kang C, Lee C, Shen J. Antimetastatic activity of novel ruthenium (III) pyridine complexes. *Cancer Med.* 2016; 5: 2850-2860. [CrossRef]
- [43] Lin K, Zhao ZZ, Bo HB, Hao XJ, Wang JQ. Applications of ruthenium complex in tumor diagnosis and therapy. *Pharmacol.* 2018; 9: 1323. [CrossRef]
- [44] Coverdale JPC, Carron TLM, Canelon IR. Designing ruthenium anticancer drugs: what have we learnt from the key drug candidates? *Inorganics.* 2019; 7: 31. [CrossRef]
- [45] Naik RM, Verma AK, Agarwal A. Kinetic and mechanistic study of the mercury(II)-catalyzed substitution of cyanide in hexacyanoruthenate(II) by pyrazine. *Transit Met Chem.* 2009; 34: 209-215. [CrossRef]

- [46] Srivastava A, Sharma V, Singh VK, Srivastava K. A Simple and Sensitive Inhibitory Kinetic Method for the Carbocysteine Determination. *J Mex Chem Soc.* 2022; 66: 57-69. [[CrossRef](#)]
- [47] Srivastava A. Quantitative estimation of D-Penicillamine in pure and pharmaceutical samples using inhibitory kinetic spectrophotometric method. *Biointerface Res Appl Chem.* 2021; 11(4): 11404-11417. [[CrossRef](#)]
- [48] Srivastava A, Naik RM, Rai J. Ag(I)-promoted substitution of cyanide from hexacyanoferrate(ii) with pyrazine: a kinetic and mechanistic study. *Russ J Phys Chem.* 2021; 95: 2545-2552. [[CrossRef](#)]
- [49] Srivastava A, Srivastava K. An Inhibitory Kinetic Method for the Methionine Determination. *Phy Chem Res.* 2022; 10(2): 283-292.
- [50] Lineweaver H, Burk D. The determination of enzyme dissociation constants. *J Am Chem Soc.* 1934; 156: 658-666. [[CrossRef](#)]
- [51] Tinoco I, Sauer K, Wang JC. *Physical chemistry, Principles and applications in biological sciences*, fourth ed., Pearson, India 2009.
- [52] *British Pharmacopoeia*, Her Majesty's Stationary Office, London, 1995.

This is an openaccess article which is publicly available on ourjournal's website under Institutional Repository at <http://dspace.marmara.edu.tr>.